THE FORMATION OF DOUBLE WORKING SURFACES IN PERIODICALLY VARIABLE JETS

A. C. Raga[1] and J. Cantó[2]

ABSTRACT

It is a well known result that a periodic ejection variability in a hypersonic jet results in the production of a train of internal working surfaces (one working surface produced by each period of the ejection variability) travelling down the jet beam. This mechanism has been successfully applied to model the knot structures of Herbig-Haro (HH) jets. In this paper we explore the possibility of producing more than one working surface with each ejection variability period. We derive the mathematical criteria that have to be satisfied by the functional form of an ejection velocity variability that produces double working surfaces, and study a family of functions with appropriate properties.

RESUMEN

Es un resultado conocido que una expulsión variable periódica en un chorro hipersónico tiene como resultado la producción de una cadena de superficies de trabajo internas (una superficie de trabajo por cada período de la variabilidad) que viajan a lo largo del chorro. Este mecanismo ha sido exitosamente aplicado para modelar las estructuras de nudos de chorros Herbig-Haro (HH). En el presente artículo exploramos la posibilidad de producir más de una superficie de trabajo con cada período de la expulsión variable. Derivamos criterios matemáticos que deben ser satisfechos por la forma funcional de una velocidad de expulsión variable que produzca superficies de trabajo dobles, y estudiamos una familia de funciones con propiedades apropiadas.

Key Words: ISM: Herbig-Haro objects — ISM: jets and outflows — ISM: kinematics and dynamics — stars: formation

1. INTRODUCTION

Rees (1978) suggested that a time-variability in the ejection of an extragalactic jet would produce shock waves travelling down the jet beam. This idea was pursued by Wilson (1984, who presented gasdynamical simulations of ejections with a periodical variability) and Roberts (1986, who presented a momentum conserving model of a stochastic ejection). Raga et al. (1990) applied variable ejection jet models to outflows from young stars.

In the context of Herbig-Haro (HH) objects, variable jet models have proved to be quite successful, because images obtained with the Hubble Space Telescope (HST) in some cases show that knot chains along HH jets show structures similar to the "internal working surfaces" that result from ejection velocity variability. Comparisons between predictions from numerical simulations of variable jets and observations have proved to be quite successful at least for some HH objects (e.g., HH 211: Völker et al. 1999; HH 111: Masciadri et al. 2002; HH 444: Raga et al. 2010; HH 34: Raga et al. 2012 HH 1: Hansen et al. 2016).

Theoretical work on variable HH jets includes both analytical models (e.g., Raga & Kofman 1992; Smith et al. 1997; Cantó et al. 2000) and numerical simulations (e.g., Stone & Norman 1993; Raga & Biro 1993; Cerqueira & de Gouveia Dal Pino 2001; Hansen et al. 2015); single- and multi-mode periodical ejections (e. g., Raga & Noriega-Crespo 1998; Raga et al. 2015), as well as stochastic ejections (Raga 1992; Yirak et al. 2009, 2012; Bonito et al. 2010a, b; Raga & Noriega-Crespo 2013; Hansen et al. 2015, 2016).

---

[1]Instituto de Ciencias Nucleares, UNAM, México.
[2]Instituto de Astronomía, UNAM, México.

Multi-mode, periodical ejection variabilities and stochastic ejections produce two-shock "internal working surfaces" which travel at different velocities along the jet beam. This results in "knot merging" events, in which a faster working surface catches up with a slower one, and both merge into a single working surface (travelling at an intermediate velocity).

A single-mode sinusoidal ejection velocity variability produces one working surface per ejection period. These successive working surfaces have almost identical time evolutions, so that catching-up events (between successive knots) do not occur. However, it is possible to construct single-mode ejection velocity variabilities which lead to the formation of two or more internal working surfaces per ejection period. These working surfaces do not necessarily have identical time evolutions, so that catching-up events can be produced.

In the present paper, we describe ejection velocity variabilities that lead to the formation of two working surfaces per ejection period. In § 2, we describe the formation of internal working surfaces by a periodic ejection velocity variability, derive criteria for the production of multiple working surfaces per ejection period, and describe possible ways to derive ejection variabilities leading to multiple working surfaces. In § 3, we explore the formation of pairs of internal working surfaces through an ejection velocity variability of the form $u_0 \propto \sin^n \omega\tau$, where u_0 is the time-dependent ejection velocity, n is an odd integer, τ is the ejection time, and ω is a constant. Finally, we summarize our results and discuss the implications for HH jets in § 4.

2. THE FORMATION OF MULTIPLE WORKING SURFACES BY A PERIODIC VARIABILITY

Let us consider a hypersonic, free-streaming jet with a time-dependent ejection velocity $u_0(\tau)$ (given as a function of the ejection time τ). As shown by Raga et al. (1990), if the ejection velocity increases with τ (i.e. $\dot{u}_0 = du_0/d\tau > 0$), the fluid parcels ejected at a time τ catch up with each other at a time

$$t_{col} = \frac{u_0}{\dot{u}_0} + \tau \,, \qquad (1)$$

(see equation 4 of Raga et al. 2015). Therefore, the parts of the $u_0(\tau)$ variability with $\dot{u}_0 > 0$ can in principle give rise to discontinuities (which correspond to two-shock "internal working surfaces", see, e.g., Kofman & Raga 1992). However, the fluid parcels ejected at a time τ can hit an already existing internal working surface at a time $t < t_{col}$.

Because of this, Raga & Kofman (1992) argued that the working surfaces corresponding to the successive ejection variability periods would initially be formed by the fluid parcels ejected at times τ_c that correspond to minima of the $t_{col}(\tau)$ function (see equation 1). Therefore, the fluid parcels which lead to the initial formation of a working surface are ejected at times τ_c which are given by the roots of the equation

$$\frac{dt_{col}}{d\tau} = \frac{d}{d\tau}\left(\frac{u_0}{\dot{u}_0}\right) + 1 = 0 \,, \qquad (2)$$

where care must be taken to see that the roots actually correspond to minima (rather than maxima) of $t_{col}(\tau)$.

For the well studied case of a sinusoidal ejection velocity variability, each period has a single root (see equation 2), and a single working surface is formed per ejection variability period (this problem having a full analytic solution, see Cantó et al. 2000). The successive working surfaces (one per ejection period) are formed at times:

$$t_c = \frac{u_0(\tau_c)}{\dot{u}_0(\tau_c)} + \tau_c \,, \qquad (3)$$

(obtained setting $\tau = \tau_c$ in equation 2) and at a distance

$$x_c = (t_c - \tau_c)\, u_0(\tau_c) \,, \qquad (4)$$

from the outflow source (see equations 7-8 of Raga et al. 2015).

It is possible to construct functional forms for $u_0(\tau)$ that produce two or more roots for equation (2) per ejection period. Let us assume that we have two roots $\tau_{c1} < \tau_{c2}$. The fluid parcels ejected around $\tau_{c,1}$ will produce a working surface at a time $t_{c,1}$ and position $x_{c,1}$ (obtained from equations 3-4). The parcels ejected around $\tau_{c,2}$ ($> \tau_{c,1}$, see above) will catch up with each other at a later time $t_{c,2}$, at a distance $x_{c,2}$ from the source (see equations 3-4).

Clearly, if

$$x_{c,2} \leq x_{c,1} \,, \qquad (5)$$

the second working surface will indeed be formed before the fluid parcels ejected at time τ_2 hit the first working surface (produced by the parcels ejected at time τ_1). Therefore, if we have a periodic ejection velocity variability $u_0(\tau)$ with two τ_c roots of equation (2) per ejection period satisfying condition (5), two internal working surfaces (per period) will be formed. These internal working surfaces will in principle have different equations of motion (resulting in different velocities along the jet flow), so that catching up processes between successive working surfaces will occur farther along the jet beam.

Of course, we could have variabilities which do not satisfy condition (5) but still lead to the formation of working surface pairs. This is due to the fact that at the time $t = t_{c,2}$ (in which the second working surface is formed) the first working surface will have moved down the jet flow from the position $x_{c,1}$ at which it was formed, to a position $x_1(t_{c,2})$. Therefore, the second working surface would still be formed provided that

$$x_{c,2} < x_1(t_{c,2}) \,. \qquad (6)$$

In order to apply this condition, however, one needs to solve the equation of motion for the first working surface (in order to calculate its position at time $t_{c,2}$). In the present paper, we will use the simpler criterion given by equation (5) (which is a sufficient but not necessary condition for the formation of working surface pairs), and apply it to study a family of periodic functional forms for $u_0(\tau)$ (see § 3).

We end this discussion by noting that it is possible to construct forms for $u_0(\tau)$ which lead to the formation of two or more internal working surfaces per ejection period in the following way. In Figure 1, we show an ejection velocity variability with two steps (at ejection times τ_1 and τ_2) of increasing velocities per ejection period p. This variability gives two roots of equation (2) which are τ_1 and τ_2. Each of these velocity jumps produces a working surface at the ejection point (i.e., $x_{c,2} = x_{c,1}$, so that condition 5 is satisfied). Therefore, two working surfaces are produced per ejection period for the velocity variability shown in Figure 1. At later times, the faster, second working surface eventually catches up with the first working surface produced by each ejection variability period.

The ejection variability shown in Figure 1 can be used as a model for obtaining continuous forms of $u_0(\tau)$ which produce two or more working surfaces per ejection period. An example of this is explored in the following section.

It is of course possible to construct a periodic ejection variability that produces two working surfaces, with the second working surface being slower than the first one. In this case, one would obtain interactions between working surfaces produced in contiguous ejection variability periods. However, by appropriately shifting the starting times of the ejection variability periods, the problem can be converted into the "slow first working surface/fast second working surface" case described above.
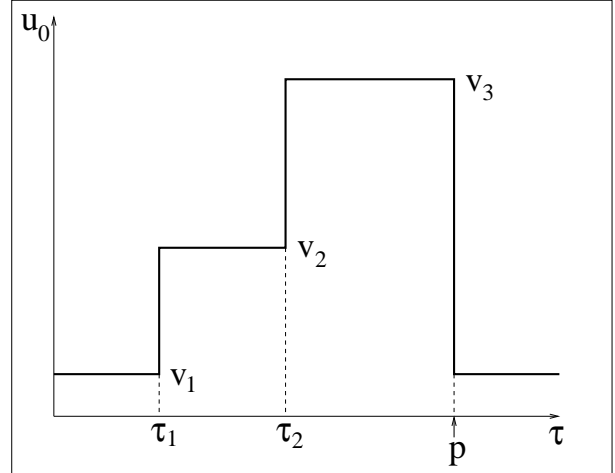

Fig. 1. Schematic diagram of a "double box-car" ejection velocity variability. Within the ejection period p, the velocity has an initial value v_1, then jumps to v_2, to v_3 and back to v_1. The properties of the resulting flow are described in § 2.

3. ODD POWERS OF A SINE WAVE

3.1. *General considerations*

We consider an ejection velocity variability of the form:

$$u_0(\tau) = v_0 + v_1 \sin^n \omega\tau \,, \qquad (7)$$

where u_0 is the ejection velocity (as a function of the ejection time τ), n is an odd integer, and v_0, v_1 and ω are constants.

In Figure 2, we show the first period of $\sin^n \omega\tau$ for $n = 1$, 3 and 5. One sees that starting from $n = 3$, this function has two steep rises (as a function of increasing $\omega\tau$) per period $p = 2\pi/\omega$. In the following subsections, we show that these two rises result in the production of a pair of internal working surfaces per ejection period.

We calculate the ejection times τ_c which give rise to the fluid parcels which eventually form internal working surfaces as the roots of equation (2). Combining equations (7) and (2) we obtain that the ejection times τ_c giving rise to working surfaces for a $\sin^n \omega\tau$ variability are given by the roots of:

$$\lambda \left(\sin^2 \omega\tau_c - 2 \right) - \sin \omega\tau_c = 0 \,, \qquad (8)$$

for $n = 1$, and

$$\lambda \left[n \sin^{n+2} \omega\tau_c - (n+1) \sin^n \omega\tau_c \right]$$
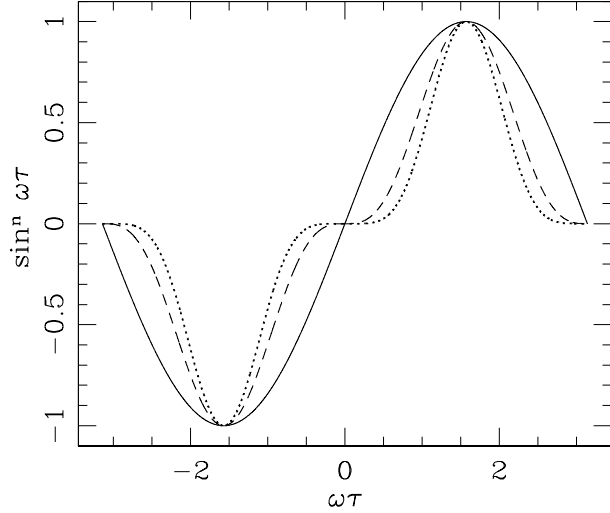$$- n \sin^2 \omega\tau_c + n - 1 = 0 \,, \qquad (9)$$

Fig. 2. This graph shows a single period of the functions $\sin \omega\tau$ (solid line), $\sin^3 \omega\tau$ (dashed line) and $\sin^5 \omega\tau$ (dotted line).

for $n = 3$, 5, ..., where $\lambda \equiv v_1/v_0$. The roots for the $n = 1$ case (equation 8) are described in § 3.2, and approximate solutions for the $n \geq 3$ case are presented in § 3.3.

3.2. The $n = 1$ case

Equation (8) has a single root

$$\sin \omega\tau_c = \frac{1}{2\lambda}\left(1 - \sqrt{8\lambda^2 + 1}\right),\qquad (10)$$

in the $-1 \leq \sin \omega\tau_c \leq 1$ range. This equation was first derived by Raga & Cantó (1998).

The values of τ_c for variabilites with $\lambda \ll 1$ can be obtained expanding equation (10) in a Taylor series to first order in λ, giving:

$$\sin \omega\tau_c = -2\lambda.\qquad (11)$$

The relevance of the $\lambda \ll 1$ regime for observed HH jets is discussed in § 5.

3.3. The case with $n \geq 3$

Solving equation (9) requires finding the roots of a polynomial of order $n + 2$ in $\sin \omega\tau_c$, so that a general analytic solution is not found. However, a straightforward, approximate analytic solution valid for small values of $\lambda = v_1/v_0$ can be obtained as follows.

In the $\lambda \to 0$ limit, from equation (9), we find

$$\sin \omega\tau_{c,0} = \pm\sqrt{\frac{n-1}{n}}.\qquad (12)$$

Now, for non-zero (but small) λ we propose roots of the form

$$\sin \omega\tau_c = \sin \omega\tau_{c,0} + h,\qquad (13)$$

with $h \ll \sin \omega\tau_{c,0}$. Substituting this proposed solution into equation (9) and expanding the powers of $\sin \omega\tau_c$ to first order in h, we find that

$$h = \frac{2\lambda s_c^{n-1}}{\lambda n(n+2)s_c^n - \lambda n(n+1)s_c^{n-2} - 2n},\qquad (14)$$

where $s_c = \sin \omega\tau_c$. We now expand equation (14) to first order in λ to obtain

$$h = -\frac{\lambda \sin^{n-1} \omega\tau_{c,0}}{n}.\qquad (15)$$

Finally, combining equations (12), (13) and (15) we obtain the roots of equation (9):

$$\sin \omega\tau_c = \pm\sqrt{\frac{n-1}{n}}\left[1 \mp \frac{\lambda}{n}\left(\frac{n-1}{n}\right)^{n/2-1}\right],\quad (16)$$

valid for small velocity amplitude to mean velocity ratios $\lambda = v_1/v_0$ (see equation 7).

3.4. Initial positions of the working surfaces

The two roots of equation (9), with the small $\lambda = v_1/v_0$ limits given by equation (16), give the ejection times of fluid parcels which lead to the possible formation of working surfaces. For the two working surfaces to be actually formed, additionally condition (5) or the less restrictive condition (6) have to be satisfied. From equations (3), (4) and (7), we see that in the small λ limit the two working surfaces are produced at distances given by

$$x_c = \frac{v_0(1 + 2\lambda \sin^n \omega\tau_c)}{n\lambda\omega \cos \omega\tau_c \sin^{n-1} \omega\tau_c},\qquad (17)$$

calculated with the negative and positive values of $\sin \omega\tau_c$ given by equation (16).

The first working surface produced by an ejection variability period (see Figure 2 and equation 7) corresponds to the negative value of $\sin \omega\tau_c$, and the second working surface to its positive value (see equation 16). From equation (17) we see that the first working surface is then formed (at a distance x_1) closer to the source than the second working surface (at a distance $x_2 > x_1$), so that the condition of equation (5) is not satisfied. However, the difference $x_2 - x_1 = (4/n\omega)|\tan \omega\tau_c|$ satisfies the condition $x_2 - x_1 \ll x_1$, x_2 (remembering that we are in the

small λ regime). Therefore, the less restrictive condition given by equation (6) is likely to be satisfied regardless of the details of the equation of motion for the first working surface.

In the following section, we present numerical solutions of Burgers' equation showing the formation of working surface pairs, and the later mergers between them.

4. NUMERICAL SOLUTIONS FOR THE $n = 3$ CASE

In order to illustrate the characteristics of a jet with "double working surfaces", we have obtained a numerical solution of Burgers' equation:

$$\frac{\partial u}{\partial t} + u\frac{\partial u}{\partial x} = 0\,, \qquad (18)$$

subject to an inflow condition

$$u_0(t) = 1 + 0.1\sin^3 t\,, \qquad (19)$$

at $x = 0$ (the outer boundary of the simulation being a free outflow). This variability corresponds to equation (7) with $n = 3$, $v_0 = 1$, $v_1 = 0.1$ and $\omega = 1$.

Burgers' equation corresponds to a pressure-less flow, and has discontinuities that correspond to two-shock working surfaces in the Euler equations. The equation of motion of the discontinuities of Burgers' equation corresponds to a ram-pressure balance working surface in a constant density flow (see, e.g., Raga et al. 1990 and Raga & Kofman 1992), and therefore generally does not agree with the motion of a working surface modeled with the gas-dynamic (Euler) equations. However, solutions of Burgers' equation do illustrate the general properties of the corresponding gasdynamic problems (in the case of hypersonic flows).

We first use equations (16) and (17) to obtain estimates for the distances from the source at which the working surfaces are formed. With the parameters of the chosen ejection velocity variability (see equation 19), we obtain a position $x_1 = 7.86$ and $x_2 = 9.72$. We can compare the results of the numerical simulation with these predictions.

The velocity structure resulting from the numerical simulations is shown in Figure 3 for different integration times. It is clear that two discontinuities (corresponding to internal working surfaces) are formed per ejection period. In the $t = 36$ velocity structure (first frame of Figure 3), we see that the first discontinuity (from one of the ejection periods) has been formed at a position $x \approx 7.5$, and in the $t = 40$ structure (bottom frame of Figure 3), we see
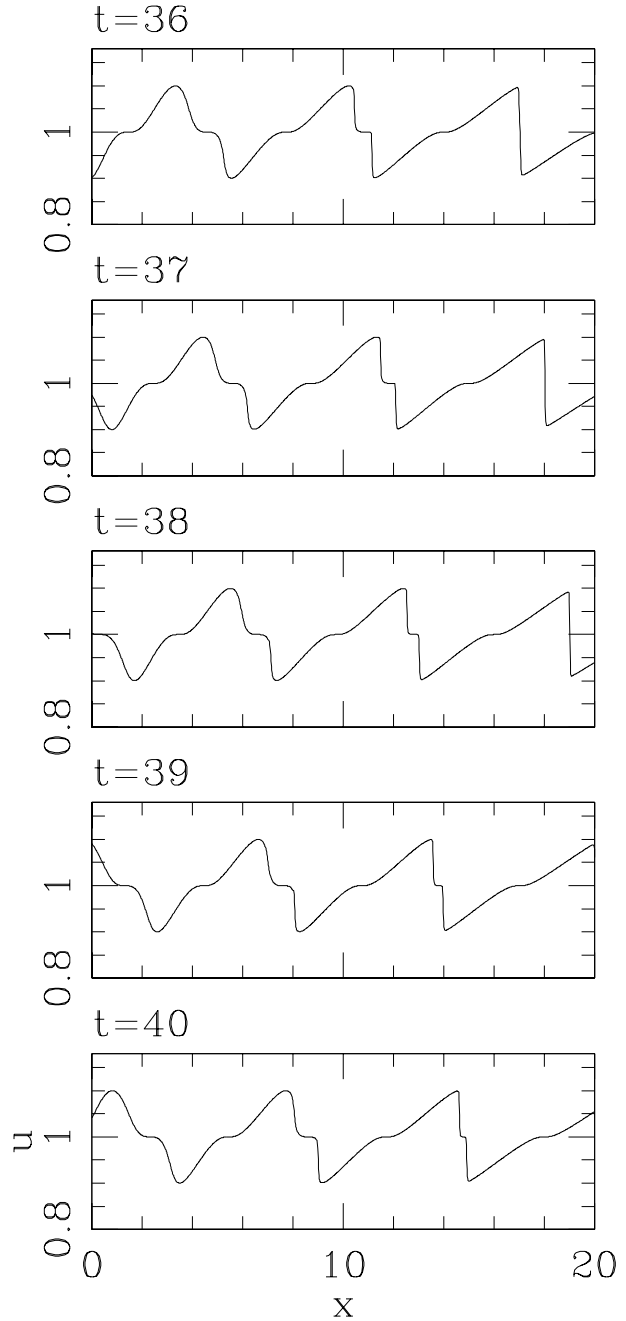

Fig. 3. This graph shows the velocity vs. position obtained at different times from a numerical solution of Burgers's equation with an ejection velocity (at $x = 0$) of the form $u_0 = 1 + 0.1\sin^3 t$. The development of double working surfaces, and the subsequent catching-ups between the working surface pairs are clearly seen.

the second discontinuity forming at $x \approx 9$. These values are in approximate agreement with the predictions from the analytic model (see above).

In the $t = 40$ velocity structure (bottom frame of Figure 3), we also see that the two working surfaces produced by one of the ejection periods (at a position $x \approx 14$) are about to merge. At larger distances from the source, we see discontinuities that correspond to merged pairs of working surfaces (see the last discontinuity of the $t = 36$, 37 and 38 velocity structures in Figure 3).

5. SUMMARY

We have explored the possible formation of multiple working surfaces in jets per ejection period of a periodic ejection velocity variability. Given the functional form of a proposed ejection velocity variability, it is clear that it produces double working surfaces if it has two roots of equation (2) which satisfy the criterion of equation (5). The ejection variability will also produce double working surfaces (per ejection period) if the roots satisfy the less stringent criterion of equation (6), but this criterion is of less straightforward application because it requires solving the equation of motion for the faster working surface (see § 2).

We have then studied a variability of the form $u_0(\tau) = v_0 + v_1 \sin^n \omega\tau$ (with odd n, see § 3), and found that for $n \geq 3$ one obtains two roots of equation (2), and that these two roots asymptotically approach the criterion of equation (5) for small values of $\lambda = v_1/v_0$. We derived approximate analytic expressions for these roots and for the distances from the source at which the resulting working surfaces are formed.

This "small λ" approximation is in principle valid for some of the knot structures observed along HH jets. Examples of this are the chains of aligned knots observed at distances of $\approx 10^{17}$ cm from the source in HH 34 and HH 111, which for an interpretation in terms of a variable jet model require amplitudes of $\approx 10\%$ of the mean velocity of the ejection (see Raga et al. 2002). As shown in § 4, for $\lambda = 0.1$ the analytic, small λ solution (described in § 3.2 and 3.3) already gives good results.

We finally presented a numerical solution of Burgers's equation for a one-dimensional flow with an ejection velocity variability of the form $u_0(\tau) = 1 + 0.1 \sin^3 \omega\tau$. In this flow, we saw that two working surfaces are formed per ejection period, at the distances from the source predicted from the analytic model.

In this numerical example, the two working surfaces that were produced have different velocities, and therefore the faster working surface catches up with the slower working surface as they travel away from the source. The position at which this catching up process occurred was approximately twice the distance from the source at which the working surfaces were formed. At larger distances from the source, one has single working surfaces (produced through the merger of the double working surfaces resulting from the ejection) per ejection velocity variability period.

This characteristic is a general feature of double working surfaces produced by periodic ejection variabilities: they only remain double working surfaces for a certain time, and eventually merge into one, as the faster working surfaces catch up with the slower ones. Therefore, one would expect to see a qualitative difference between the knot structures at larger distances from the source (where we see merged knots) and close to the point of working surface formation (where we see the double working surfaces). Such an effect has been described by Raga & Noriega-Crespo (2013) for the HH 34 jet, but no comparable studies exist for other HH objects.

Because of this lack of clear application, our present work should be regarded as a mathematical curiosity relating to the formation of shock structures in periodically variable jets. The method which we have described for evaluating the possible formation of double working surfaces (per ejection period) might be useful for choosing appropriate forms for an ejection velocity when trying to simulate specific HH jets.

An interesting question is whether or not the analytic approach used in this paper is applicable to the case of magnetized jets. The criterion for working surface formation (see § 2) is valid for a ballistic flow. In the case of a magnetized jet, a ballistic regime is obtained if the flow is hypersonic and also "hyperalfvénic" (i.e., with a jet velocity much larger than the Alfvén velocity). Therefore, under these conditions the analysis presented above should also be valid. However, implicit in the discussion of the subsequent evolution of the working surfaces (involving "catching up" events) is the assumption that they have a small spatial extent along the outflow axis (i.e., that the two shocks in the working surfaces have relatively small separations). This is not necessarily the case for magnetized jets, which (depending on the radial configuration of the magnetic field) can have internal working surfaces with substantial axial extents (see, e.g., De Colle et al. 2008 and Hansen et al. 2015). If this axial stretching is large enough, it can also lead to mergings between successive working surfaces. This effect (which is nicely illustrated in Figure 2 of Hansen et al. 2015 for

the case of axisymmetric, magnetized jets) was studied (for the case of 1D, non-magnetized flows, which also develop axially extended working surfaces) by Smith et al. (1997). Clearly, variable jets with axially extended, double working surfaces (which could be obtained with one of the ejection variabilities discussed above, together with an appropriate magnetic field configuration) will have a richness of behaviour not appropriately described by the simple, "catching up" description which we have used in the present paper.

REFERENCES

Bonito, R., Orlando, S., Peres, G., et al. 2010a, A&A, 511, 42
_____. 2010b, A&A, 517, 68
Cantó, J., Raga, A. C., & D'Alessio, P. 2000, MNRAS, 313, 656
Cerqueira, A. H. & de Gouveia Dal Pino, E. M. 2001, ApJ, 560, 779
De Colle, F., Raga, A. C., & Esquivel, A. 2008, ApJ, 689, 302
Hansen, E. C., Frank, A., & Hartigan, P. 2015, ApJ, 800, 41
Hansen, E. C., Frank, A., Hartigan, P., & Lebedev, S. V. 2016, ApJ, in press
Kofman, L., & Raga, A. C. 1992, ApJ, 390, 359
Masciadri, E., Velázquez, P. F., Raga, A. C., Cantó, J., & Noriega-Crespo, A. 2002, ApJ, 573, 260
Raga, A. C. 1992, MNRAS, 258, 301
Raga, A. C. & Biro, S. 1993, MNRAS, 264, 758
Raga, A. C. & Cantó, J. 1998, RMxAA, 34, 73
Raga, A. C., Cantó, J., Binette, L., & Calvet, N. 1990, ApJ, 364, 601
Raga, A. C. & Kofman, L. 1992, ApJ, 386, 222
Raga, A. C. & Noriega-Crespo, A. 1998, AJ, 116, 2943
_____. 2013, RMxAA, 49, 363
Raga, A. C., Riera, A., & González-Gómez, D. I. 2010, A&A, 517, A20
Raga, A. C., Rodríguez-Ramírez, J. C., Cantó, J., & Velázquez, P. F. 2015, MNRAS, 454, 412
Raga, A. C., Rodríguez-González, A., Noriega-Crespo, A., & Esquivel, A. 2012, ApJ, 744, L12
Rees, M. J. 1978, MNRAS, 184, 61
Roberts, M. R. 1986, ApJ, 300, 568
Smith, M. D., Suttner, G., & Zinnecker, H. 1997, A&A, 320, 325
Stone, J. & Norman, M. L. 1993, ApJ, 413, 210
Völker, R., Smith, M. D., Suttner, G., & Yorke, H. W. 1999, A&A, 343, 953
Wilson, M. J. 1984, MNRAS 216, 923
Yirak, K., Frank, A., Cunningham, A. J., & Mitran, S. 2009, ApJ, 695, 999
Yirak, K., Schroeder, E., Frank, A., & Cunningham, A. J. 2012, ApJ, 746, 133

J. Cantó: Instituto de Astronomía, Universidad Nacional Autónoma de México, Ap. 70-468, 04510, Ciudad de México, México.
A. C. Raga: Instituto de Ciencias Nucleares, Universidad Nacional Autónoma de México, Ap. 70-543, 04510, Ciudad de México, México (raga@nucleares.unam.mx).